Computers and Electronics in Agriculture 167 (2019) 105019

Contents lists available at ScienceDirect

Computers and Electronics in Agriculture

journal homepage: www.elsevier.com/locate/compag

Methodology for data processing and analysis techniques of infrared video thermography used to measure cattle temperature in real time

Holly Cuthbertson[a,c,*], Garth Tarr[a,b], Luciano A. González[a,c]

[a] The University of Sydney, Sydney Institute of Agriculture, Sydney, NSW 2006, Australia
[b] The University of Sydney, School of Mathematics and Statistics, Sydney, NSW 2006, Australia
[c] The University of Sydney, School of Life and Environmental Sciences, Centre for Carbon, Water and Food, Camden, NSW 2570, Australia

ARTICLE INFO

Keywords:
Infrared thermography
Rectal temperature
Region of interest
Beef cattle
Video camera

ABSTRACT

Core body temperature is a measurement used to evaluate and diagnose the health status of cattle, with rectal temperature measured using an indwelling probe being the preferred method. This procedure can be stressful to animals, potentially generating inaccurate results and is impractical. Infrared thermography (IRT) of the ocular region of the eye in cattle may be a less stressful and safer alternative. The objective of the present study was to develop a method to measure the temperature of cattle using IRT under commercial settings. One-hundred and twenty cattle, of mixed breeds were used in Experiment 1 and were recorded by 3 different IRT cameras placed on the race in a commercial abattoir. Experiment 2 used 52 cattle of mixed breeds that were recorded by 4 different IRT cameras at the same sample place and distance from the cattle crush on a farm. Animals in Experiment 2, were caught in the crush where IRT data and rectal temperature was recorded. Under commercial abattoir conditions, IRT data shows large variability ranging from 23.1° to 47.5 °C, calling for extensive data processing. When the eye was within the region of interest (ROI) under commercial conditions it reflected the highest temperature in comparison to the skin or facilities. The maximum temperature within the ROI was extracted from the frames containing the ocular region of the eye (raw data) and then these data processed, calculating the rolling median and quantiles. The correlation between eye IRT and rectal temperature is lower when using unprocessed raw data ($r = 0.19$; $P > 0.05$) compared to using quantiles or the rolling median ($r = 0.43$; $P < 0.05$) due to the presence of outliers. The frame rate, image resolution and accuracy of the cameras also affected the correlation between eye IRT and rectal temperature. This resulted in some data processing methods that worked well for some cameras but not for others. Reducing the length of time animals were within the ROI produced a reduction in the strength of the correlation between IRT eye and rectal temperature. However, some cameras such as the FLIR A310 were less affected by the length of time. We demonstrate that a 1-second rolling median of the maximum and the 99th quantile is an appropriate methodology to analyse IRT data collected at a high frequency using video cameras. Data from video IRT cameras require extensive processing before it can be used to measure body temperature in cattle under commercial conditions.

1. Introduction

A common method used to monitor the health status of animals or responses to external stimuli and stress involves measuring core body temperature (Herborn et al., 2015; Knížková et al., 2007; Mccafferty, 2007). Measuring rectal temperature with an indwelling digital thermometer has been the most widely used method to date, however this approach is time-consuming, disruptive and only gives a single temperature reading (Burfeind et al., 2010; Sellier et al., 2014). Due to the animal needing to be restrained to obtain rectal temperature, this method is likely to invoke a stress response, which could result in stress induced hyperthermia and hence would decrease the accuracy of the measurement (Naylor et al., 2012). Furthermore, it is known that rectal temperature is more stable and less reactive to external stimuli than body surface temperature (George et al., 2014).

The need for more sensitive methods has led to the development of new technologies such as subcutaneously implanted transmitters, intravaginal loggers and rumen boluses, which allow for continuous remote recording of core body temperature over longer periods of time (Koltes et al., 2018; Rose-Dye et al., 2011; Wacker et al., 2012). These

* Corresponding author at: The University of Sydney, School of Life and Environmental Sciences, Centre for Carbon, Water and Food, Camden, NSW 2570, Australia.

E-mail address: holly.cuthbertson@sydney.edu.au (H. Cuthbertson).

https://doi.org/10.1016/j.compag.2019.105019
Received 28 March 2019; Received in revised form 24 June 2019; Accepted 19 September 2019

technologies show promise for certain applications, but they are still invasive; requiring restraint of the animal and, as with rectal temperature measurement, often encounter problems associated with device retrieval (Sellier et al., 2014). Additionally, data from these devices are often not available in real time, with data only available after device retrieval, or require one sensor for each animal. In technologies where real time data transmission is possible, there are often issues surrounding battery life and signal strength that hamper the ability to provide data in real time (Herborn et al., 2015). Therefore, there is a need for less invasive, more efficient methodologies to determine the temperature of animals in a continuous, precise, simple and automated fashion. Ideally, this methodology should be provided at a low cost per animal to be practical under commercial conditions such as farms or abattoirs.

Infrared thermography (IRT) is becoming a widely used technique to remotely measure the surface temperature of objects (McManus et al., 2016). When subjects cannot be captured, body temperature patterns can be studied using IRT (Mccafferty, 2007; Salles et al., 2016). Infrared cameras measure the amount of heat emitted from an object and converts this information into a thermal image (thermogram) (Mccafferty, 2007). The IRT devices are able to measure the fluctuations in blood flow and heat transfer by detecting the small changes in the animals' body temperature (Schaefer et al., 2004). The IRT technology may be useful as a potential indicator of stress in animals because of its ability to detect heat production and loss from animals (Stewart et al., 2005). Infrared thermography was initially developed in 1800, and the basis of IRT theory has been well explained and documented (Wolfe, 1965). IRT has shown promising results in the detection of inflammation and injury in animals (Knížková et al., 2007; Stewart et al., 2005) and cases of disease in humans (Lahiri et al., 2012). Despite these potential advantages, the efficacy of ocular video IRT to measure core body temperature in cattle and a methodology to process such data have not yet been published. A wide range of IRT cameras and devices are commercially available, however, data collected can differ between technologies due to differences in frame rate (Hz or photograms per second), sensitivity and image resolution which is the size and number of pixels within the image that ultimately controls image quality (Usamentiaga et al., 2014). IRT data is also very variable and extremely sensitive to environmental conditions (Church et al., 2014). As a result, IRT data can be very noisy, contain erroneous data and produce inaccurate results if steps are not taken to ensure a robust methodology for analysis.

Most IRT studies use the temperature of the pixel with the maximum temperature within a region of interest (ROI) or frame (Hoffmann et al., 2013; Salles et al., 2016; Stewart et al., 2007) or a combination of maximum values such as the average of several pixels with maximum values (Ludwig et al., 2014; Šabec and Lazar, 1990). Most previous animal studies using IRT cameras have used still images to estimate body temperature from this maximum value within a ROI (Gariepy et al., 1989; Schaefer et al., 2004). Hoffmann et al. (2013) utilised the top 10 maximum IRT values over a period of 7 min for analysis. However, due to time constraints and real time application, this approach is impractical from a commercial standpoint and there are concerns around the effect of outliers on the results. The temperature of the pixel with maximum temperature is most commonly used because of the ease to calculate using IRT software where the user can create a ROI on the animal (e.g. eye, back of ear, hind legs) and obtain the temperature of the pixel with the maximum value within that ROI. Furthermore, the ocular region of the eye has consistently shown to be the best anatomical location for the early detection of response to stress and disease (Bartolomé et al., 2013). The ocular area in the eye of animals is a very responsive location due to high blood flow in the surface from capillary vessels and it's close proximity to the brain (Church et al., 2014; Kessel et al., 2010). Additionally, the ocular area in the eye also has the highest temperature of the animal, closest to that of rectal temperature, and is the easiest and quickest to obtain in an automatic monitoring system (George et al., 2014; Kessel et al., 2010). In IRT data, outliers are likely to appear due to factors such as head movement of the animal and the maximum value may no longer be an accurate representation of the animals' surface temperature. Hence, robust methods for data processing of video IRT containing outliers are required to process high frequency data collected under commercial conditions. In addition, latest IRT video cameras collect frames at very fast rates (up to 1000 images per second) which poses a challenge for data processing and analysis.

The aims of the present study were 1) to evaluate video IRT to measure body temperature in cattle for its use under commercial situations such as abattoirs and farms, 2) to develop a methodology to analyse the data and, 3) to determine the minimum length of time collecting IRT data. The objective was addressed through two experiments. Experiment 1 measured IRT of cattle in an abattoir to understand the challenges and guide us in the development of automatic processing methods of IRT data. Experiment 2 measured the ocular (ocular area) IRT temperature of cattle using different cameras and rectal temperature as a baseline reference, to determine the most accurate data processing method.

2. Materials and methods

The Sydney University Animal Ethics Committee, in accordance with the Australian Code of Practice for the Care and Use of Animals for Scientific Purposes, approved all procedures outlined below under permit number 869 and 993.

2.1. Animal management

For Experiment 1, two infrared cameras (FLIR A310 and FLIR T420; FLIR Systems Inc., Wilsonville, Oregon) were set up inside an abattoir to record the surface temperature of cattle moving through the race leading to the knocking box. Animals moved through the race to the knocking box at commercial speed, slaughtering 60 animals per hour on average. Animals were merely observed in this experiment, with no interference from research personnel. One-hundred and twenty cattle were recorded during this experiment. Recording conditions in the abattoir differed slightly between the different cameras explained below and all recordings were conducted under sheltering from the abattoir, which reduced the effect of environmental solar radiation, temperature and relative humidity. Two infrared cameras (FLIR A310 and T420; Table 1) were placed at an angle of 45° of the race, 2 m from the animal (Fig. 1).

The animals used in Experiment 2 were Angus yearling beef cattle (n = 52). The study was conducted over 4 hours from midday on a

Table 1
Specifications of the four FLIR infrared cameras (3 video-imagery and 1 single image camera) used to measure surface temperature in cattle.

FLIR Model	Resolution	Accuracy	Sensitivity	Temperature Range	Frame rate (Hz)
A310	320 × 240	± 2 °C	0.05 °C at 30 °C	−20 °C to 120 °C	9
A65	650 × 512	± 5 °C	0.05 °C at 30 °C	−20 °C to 500 °C	10
T420	320 × 240	± 2 °C	0.045 °C at 30 °C	−20 °C to 650 °C	24
C2 (single images only)	80 × 60	± 2 °C	0.05 °C at 25 °C	−10 °C to 150 °C	1

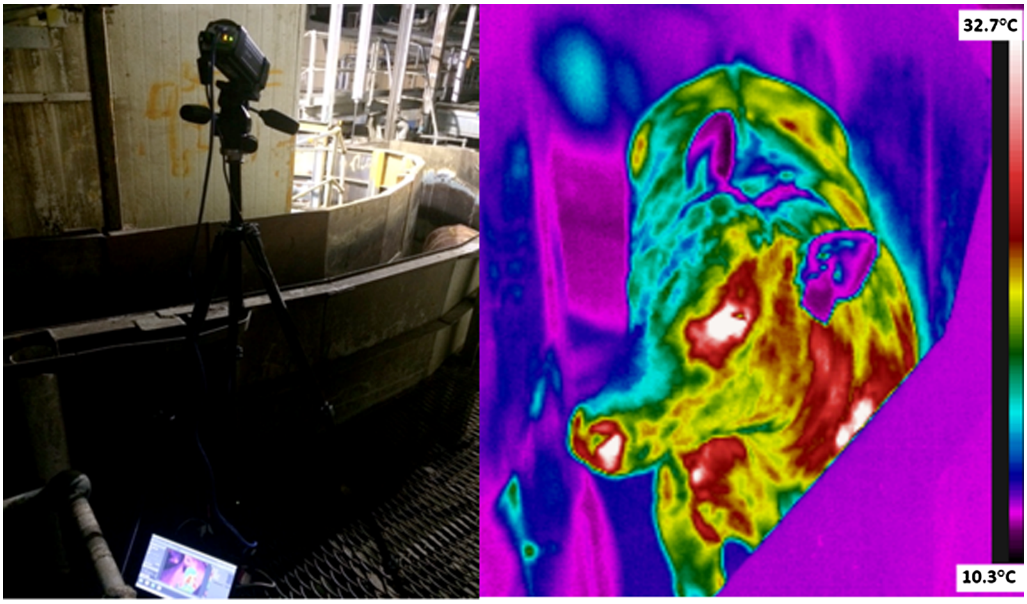

Fig. 1. Setup of infrared video cameras (left) and screenshot of video IRT footage (right; FLIR A310 camera) in the race before the knocking box at a commercial abattoir. Different colours indicate temperature ranges with white being the hottest and black being coldest.

University owned farm. On the sampling day, animals were mustered by farm staff and brought into the shaded holding yards one hour before the trial commenced, with freely available water and was approximately 4 m^2. Animals were moved through the race, into a weighing station where each animal was weighed, then released into a 2-metre race leading to a cattle crush where animals were held for approximately 5–7 min. During this time, a digital thermometer (Shoof International, Large Animal model) was used to measure rectal temperature of every animal at the beginning of every IRT video. Rectal temperature was always measured at the same insertion depth of 5 cm for 10 s, when signalled by an acoustic noise from the thermometer indicating a stable measurement occurred. Cameras were under a large shaded area that covered the race, weighing station and crush. Four different IRT cameras were used in this experiment, three recording radiometric videos (FLIR A65, A310 and T420; Table 1) and the other radiometric single still images (FLIR C2; Table 1). The A65 was the only IRT video camera used with fixed focus, whereas, the A310 and T420 have the option for either autofocus or focussing on demand by pressing a button on the software. IRT videos were taken on a 60°angle, 2 m from the camera lens to the longitudinal line of the body of the animal. The FLIR C2 camera, capturing radiometric images was manually operated, with photos taken from the same location, angle and distance as the video IRT cameras. Two images were captured for each animal with the C2. Cameras were set up to record from the exact same location, which was located perpendicular to the cattle crush so that a comparison could be made between the different cameras.

2.2. Infrared thermography processing and analysis

The ambient temperature and relative humidity, distance to object and emissivity was adjusted appropriately for all cameras in both trials. The ambient temperature and relative humidity information was obtained from Bureau of Meteorology's (BOM) Bringelly weather station and an average was calculated for the duration of the collection period in Experiment 2. Emissivity was set to 0.98 in agreement with previous studies with mammals (Bernard et al., 2013; Hoffmann et al., 2013). The cameras were configured and image data analysed using FLIR's Infrared Software (Research IR Version 4.30; FLIR Systems Inc., Wilsonville, Oregon). Data processing consisted of the following: 1) setting up a ROI that contains the ocular area of the eye of the animal when present, 2) extracting the maximum temperature within this ROI. These data contained frame number, time and temperature of the pixel with maximum value within the ROI for each frame and, 3) manually watching the videos to annotate the first and last frame number for each animal ID. For Experiments 1 and 2 approximately 14, 200 images in total were used.

In Experiment 1, the ROI was setup as a box to ensure that only one animal at a time was being measured within this ROI and that there was no presence of any background interference that could occur from machinery or abattoir personnel in the background of the ROI (Fig. 1). In addition, to annotating start and end frame number for each animal, the first 20 animals for each camera (n = 40) were analysed further by an experienced IRT person manually watching the footage to note what part of the animal was within the ROI as either the eye or the body for each animal in each frame.

In Experiment 2, all IRT cameras' ROI contained the animals head, with a clear focus on the ocular region of the eye. Animals were held in the head bail, obtaining a large number of frames per animal. However, many frames were unsuitable for analysis due the animal entering and leaving the crush, the camera refocussing or abrupt head movements from the animal resulting in the eye going outside the ROI. These frames were removed if the animal was not restrained in the crush or the eye was not within the ROI. The removal of these frames was done manually by an experienced IRT person watching the footage. This processing led to a cleaner dataset, where it was certain that the maximum IRT temperature recorded was coming from the ocular area of the eye on the animal.

2.3. Statistical analysis

For Experiment 1, temporal line plots were used to visualise the IRT temperature measurements of each animal over time, and histograms to determine temperature distribution. The raw maximum temperature was included in the analysis for both experiments. In Experiment 2, the raw maximum temperature was smoothed using the rolling median, then the rolling median time series was processed to calculate the following summary statistics for each animal: 50th, 60th, 70th, 75th, 80th, 90th, 95thand 99th quantiles (q) for each animal.

A 1-second rolling median was applied to the raw maximums from each sequence of frames as a smoothing technique used to reduce the influence of outliers in the dataset (Arce, 2005, Chapter 5). A 1-second window was chosen as it smooths over enough time to minimise the impact of short events that interfere with obtaining a representative measurement from the ocular region of the eye, for example, the animal blinking and shaking its head or other distortions such as camera refocussing. This approach is hardware adaptive, in that the smoothing window operates over a number different frames depending on the frame rate of the camera. To achieve a 1-second rolling median, in Experiment 2, the rolling median window considered 10 frames from the A65, 9 from the A310, and 24 from the T420.

After smoothing the data using a 1-second rolling median, a range of quantiles were considered in Experiment 2 to determine which one yielded most robust data against hot objects such as, equipment or personnel that entered the ROI and successfully removed the effect of occasional unexplained IRT spikes that were not smoothed over by the rolling median.

The value used for analysis from the C2 camera was calculated as the average from the maximum values of the two images for each animal.

In Experiment 2, the objective was also to determine the minimum amount of time needed for an accurate IRT temperature measurement. This was analysed by first extracting two-random non-overlapping chunks of, 1, 2, 3, 5, 10, 15 and 20 s of temperature data for each animal, then calculating the summary statistics for each of these (quantiles and rolling median), and finally calculating the correlation coefficient between any two chunks. These IRT statistics were also used to estimate Pearson correlations with rectal temperature. Small correlation was considered between ± 0.1 and 0.3, moderate ± 0.3 and 0.7 and strong if greater than ± 0.7 as recommended by Ratner (2009). P value ≤ 0.05 was chosen as the threshold for statistical significance in all tests.

R version 3.5.2 was used for all analysis (R Core Team, 2015) with visualisations created using ggplot2 (Wickham, 2016). A shiny web interface was also created to facilitate data exploration (Chang et al., 2018). The rolling median was implemented using the runquantile function from the caTools package (Tuszynski, 2019)

3. Results

3.1. Experiment 1

Summary statistics for the raw maximum IRT and the calculated statistics including, 1-second rolling median and the quantiles appear in Table 2. Mean IRT increased from the q50 (lowest) to the raw data (highest), whereas the variability across animals decreased from q50 to the raw data.

Fig. 2 shows the maximum IRT of the raw data within the ROI as animals moved through the race of the abattoir. These data also showed large variability in the temperature reading as the animals move through the race at abattoirs and the ocular area of the eye fell within the ROI (highest temperature > 32 °C; green boxes) or the skin of the body (medium temperature at approximately 27 to 30 °C; red boxes), or when no animals were within the ROI showing the lowest temperature (< 20 °C; blue boxes).

A histogram of the raw maximum IRT showed the presence of three different populations data points from a camera setup at the abattoir are plotted (Fig. 3). Each of these populations belong to 1) high temperature when the ocular area of the eye was within the ROI, 2) medium temperature when other parts of the body (skin) were within the ROI but not the eyes, and 3) low temperature when there were no animals within the ROI. In addition, IRT temperature was higher when the eye (32.6 °C ± 0.01) was within the ROI compared to IRT data when the body (30.73 °C ± 0.03) was within the ROI ($P < 0.001$; Fig. 4).

Table 2
Summary statistics of the 40 cattle analysed in detail using 2 infrared cameras to measure body surface temperature. Quantiles were calculated from the rolling median maximum series.

Summary Statistic	obs	mean	sd	median	min	max	se
50th quantile	40	29.43	3.75	28.13	23.7	37.88	0.44
60th quantile	40	29.75	3.71	28.58	23.8	37.97	0.44
70th quantile	40	30.11	3.69	28.79	24.53	38.02	0.44
75th quantile	40	30.25	3.68	28.93	24.57	38.03	0.43
80th quantile	40	30.37	3.61	28.95	24.57	38.03	0.43
90th quantile	40	30.7	3.59	29.31	24.64	38.06	0.42
95th quantile	40	30.96	3.52	30.22	24.64	38.07	0.42
97th quantile	40	31.16	3.46	30.95	24.64	38.09	0.41
99th quantile	40	31.56	3.38	31.9	24.64	38.11	0.4
Rolling median maximum	40	31.95	3.4	33.03	24.64	38.11	0.4
Raw maximum	40	32.63	3.08	33.07	27.37	38.19	0.36

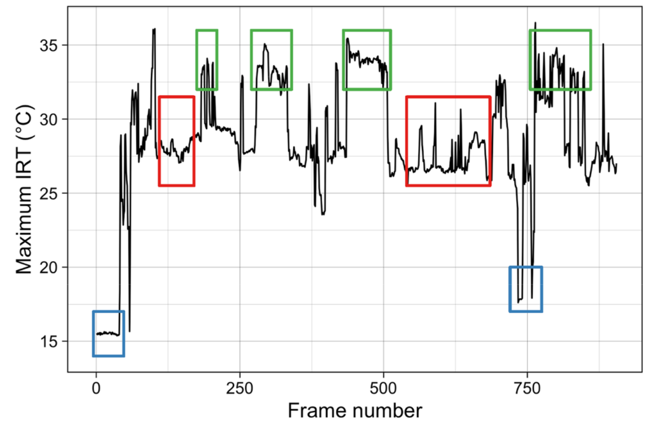

Fig. 2. Example of maximum IRT temperature within the region of interest from a video IRT camera set up in the race of an abattoir to measure cattle surface temperature over time. Green Box indicates the animals' ocular area of the eye (> 32 °C), red box indicates the animals' skin of the body (27 to 30 °C), and the blue box indicates that there is no animal (< 20 °C) within the region of interest. (For interpretation of the references to colour in this figure legend, the reader is referred to the web version of this article.)

3.2. Experiment 2

3.2.1. Data processing: smoothing method

Due to the high variability of IRT data, a rolling median was used to smooth out any sudden spikes or declines due to camera refocussing or head movement as shown in example in Fig. 5, where the rolling median has reduced the size of the spikes and troughs in the raw data. Smoothing of the raw data decreased the estimated temperature in both the A310 and T420, however, had no effect for the A65 camera (Fig. 6).

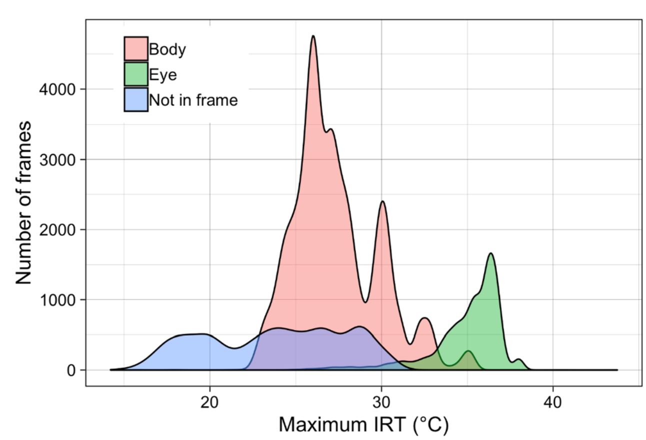

Fig. 3. Frequency distribution of infrared temperature data according to the body parts of cattle within the region of interest measured in the race of a commercial abattoir.

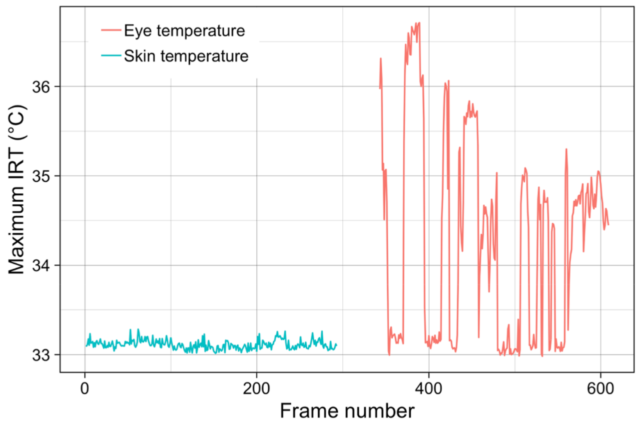

Fig. 4. Raw maximum infrared thermography series with the ocular region of the eye (red line) and the skin of the animal (blue line) within the region of interest obtained from cattle in the race prior to slaughter at a commercial abattoir. (For interpretation of the references to colour in this figure legend, the reader is referred to the web version of this article.)

3.2.2. Camera comparison and summary statistic

The data processing pipeline of the rolling median and calculation of the quantiles helped to remove cases of background interference, refocussing of the camera and erratic head movements (Fig. 5). Calculation of the quantiles from the 1-second rolling median helped to remove further cases of background interference, refocussing of the camera and erratic head movements (Fig. 5.

The quantiles in Fig. 5 are not affected by 1) when the eye is not within the field of view (Animal A) or 2) erratic head movements (Animal B). The raw maximum in Fig. 5 comes from the highest peak in the IRT data for each animal and it is not representative of the entire data collected. Pearson correlations between the IRT statistics using all data available for each animal and rectal temperature are displayed in Fig. 7 for each camera. It is important to point out that the C2 camera resulted in the lowest correlation coefficient between IRT and rectal temperature, compared to the rest of the cameras ($r = 0.22$; $p < 0.05$; data not shown). All three IRT video cameras revealed a positive correlation with rectal temperature for all summary statistics ($p < 0.05$), except for the maximum of the raw data for the cameras with auto focus ($p > 0.05$ for T420 and A310). On average across all cameras, the summary statistic chosen had small effect on the strength of the correlations, although, the q95, q97 and q99 showed slightly stronger correlations between IRT and rectal temperature. In addition, marked differences existed between cameras for some summary statistics. The A310 showed the highest correlation with rectal temperature with the q97, q99 and rolling median ($p < 0.001$; Fig. 7). The A65 camera showed the strongest correlation of all cameras with the q60, q70, q80, q90 and maximum IRT from the raw data (Fig. 7). In contrast, correlations with the T420 were slightly lower compared to the rest of the cameras and the lowest correlations with the maximum temperature from the raw data.

The highest correlation for any camera was found for the A310 camera using the maximum of the 1-second rolling median ($r = 0.57$, $p < 0.0001$) and q99 ($r = 0.56$, $p < 0.0001$).

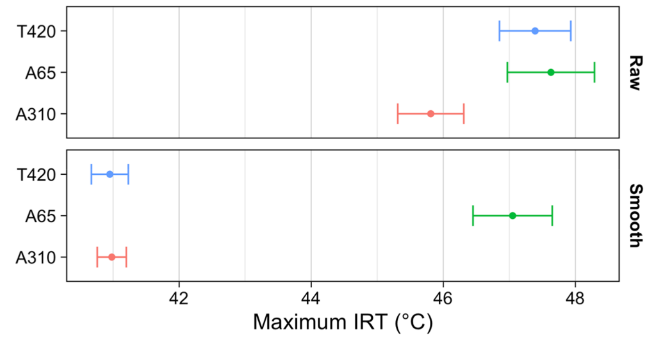

Fig. 6. Mean infrared temperatures from 3 different cameras (T420 is blue, A65 is green and A310 is red) for both raw and 1-second rolling median smoothed data recorded in cattle under commercial farming conditions. (For interpretation of the references to colour in this figure legend, the reader is referred to the web version of this article.)

3.2.3. Repeatability of measurements with different lengths of videos

The correlation between IRT temperature estimated using 1, 2, 3, 5, 10, 15 and 20 s of data for each animal with another period of data for the same animal for the 95th, 97th, 99th quantile, and the smoothed

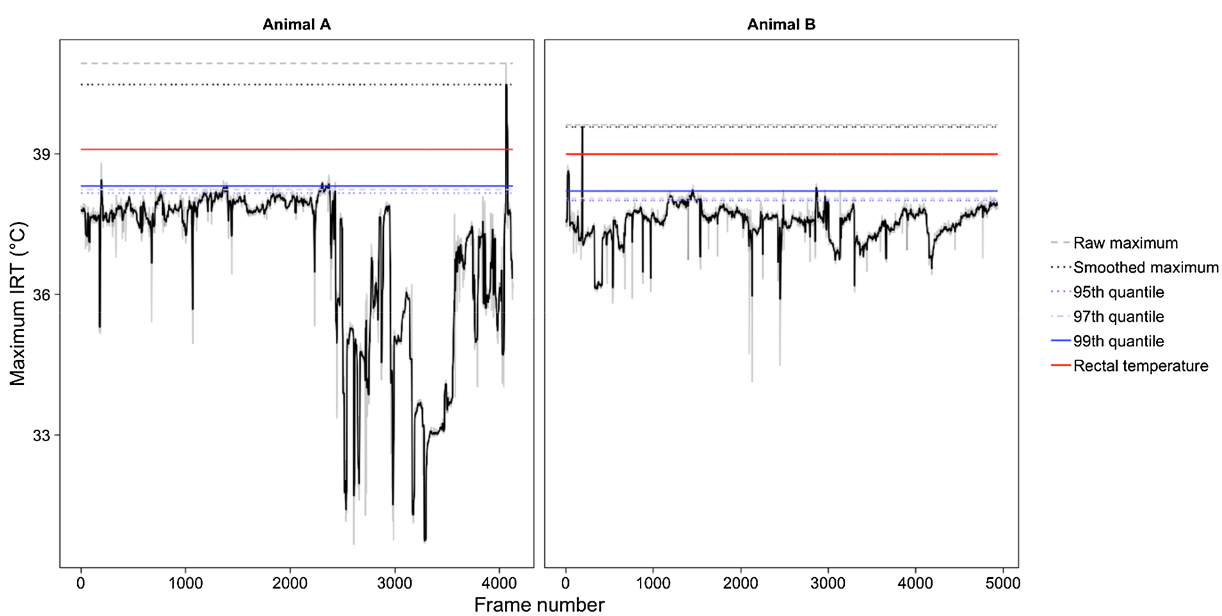

Fig. 5. Maximum IRT within the region of interest (grey line; raw data) measured on 2 animals and algorithm developed to process the data to 1) reduce the effect of the sudden spikes of high or troughs of low temperature using the 1-second rolling median (black line), and 2) obtain summary statistics for final analysis calculating quantiles (q95, q97, q99).

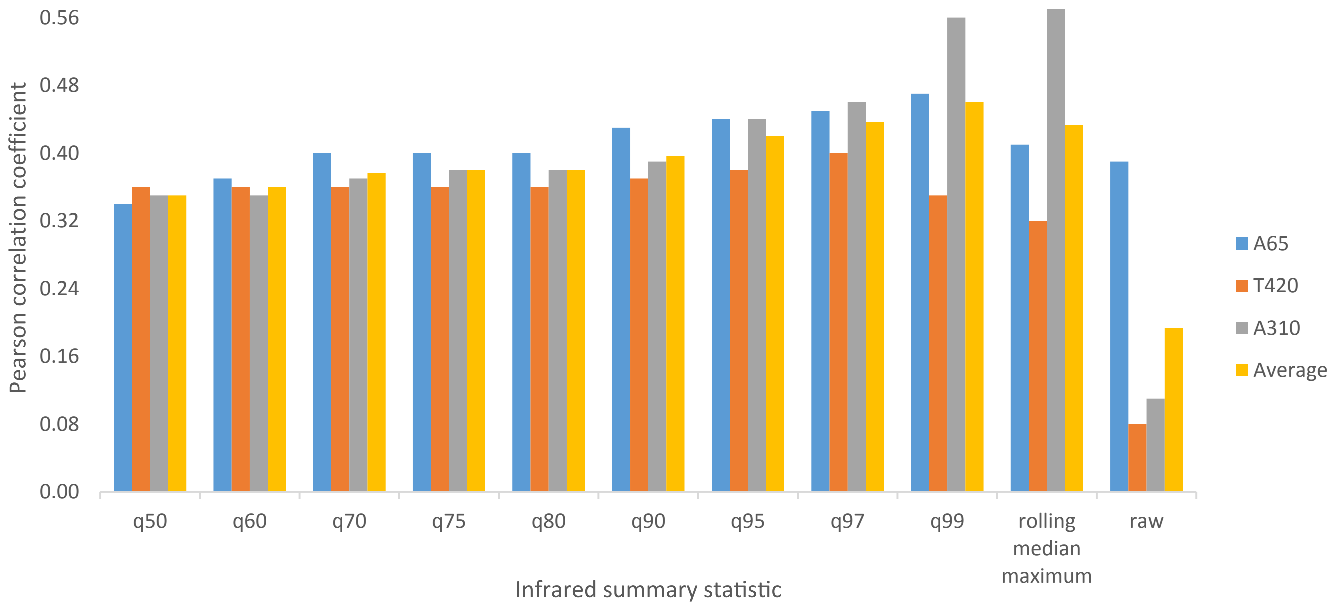

Fig. 7. Pearson correlations between rectal and eye temperature (ocular area) of cattle measured with 3 different infrared cameras (A65 is blue, T420 is orange and A310 is grey) and the average (yellow) of the 3 cameras. Where r ≥ 0.32P < 0.05. (For interpretation of the references to colour in this figure legend, the reader is referred to the web version of this article.)

maximum is shown in Tables 3, 4, 5 and 6, respectively. Correlations across cameras and summary statistics were moderate to high with an average of r = 0.66. The repeatability of the measurements was similar across statistics with average correlation coefficients being 0.703, 0.723 and 0.715 for maximum IRT from smoothed data, q97 and q99, respectively. Similarly, calculations from these tables across all cameras and summary statistics indicate that any 1-second chunk of data had an average correlation of 0.71 with any other chunk of 1, 2, 3, 5, 10, 15, 20-seconds chunk of data. Furthermore, any 20-second chunk of data showed an average correlation coefficient of 0.72 with any other non-overlapping chunk of 1, 2, 3, 5, 10, 15 or 20-seconds. In general, 1-second chunks of data with another 1-second chunk of data elsewhere for the same animal, 5 s with another 5 s chunk, and 20 s with another 20 s gave the highest correlation. The 20 and 5-seconds chunk of data showed the largest average correlations across all 3 cameras (r = 0.75 and 0.74, respectively) In terms of shorter chunks being able to predict larger chunks of data, the q95 and q97 of the A310 had the highest correlation for 3 s chunk against a 20 s chunk (0.82).

Table 3
Pearson correlations between the IRT temperatures of cattle with any two non-overlapping data time chunks for the same animal (1, 2, 3, 5, 10, 15 and 20 s) using the 95th quantile summary statistics.

	1 sec	*2 sec*	*3 sec*	*5 sec*	*10 sec*	*15 sec*	*20 sec*
A65							
1 sec	0.83						
2 sec	*0.87*	0.82					
3 sec	*0.78*	*0.82*	*0.83*				
5 sec	*0.73*	*0.76*	*0.81*	0.86			
10 sec	*0.74*	*0.75*	*0.8*	0.87	0.71		
15 sec	*0.73*	*0.78*	*0.82*	0.87	0.75	0.81	
20 sec	*0.72*	*0.76*	*0.82*	0.82	0.79	0.85	0.82
T420							
1 sec	*0.91*						
2 sec	*0.73*	*0.79*					
3 sec	*0.76*	*0.79*	*0.81*				
5 sec	0.76	0.73	0.8	0.52			
10 sec	0.64	0.63	0.64	0.68	0.65		
15 sec	0.69	0.73	0.75	0.73	0.65	0.62	
20 sec	0.64	0.67	0.74	0.75	0.63	0.61	0.69
A310							
1 sec	*0.67*						
2 sec	*0.67*	*0.69*					
3 sec	*0.7*	*0.67*	*0.61*				
5 sec	0.55	0.56	0.66	0.63			
10 sec	0.63	0.62	0.66	0.74	0.86		
15 sec	0.66	0.69	0.72	0.79	0.87	0.84	
20 sec	0.66	0.7	0.73	0.8	0.85	0.82	0.78

Table 4
Pearson correlations between the IRT temperatures of cattle with any two non-overlapping data time chunks for the same animal (1, 2, 3, 5, 10, 15 and 20 s) using the 97th quantile summary statistics.

	1 sec	*2 sec*	*3 sec*	*5 sec*	*10 sec*	*15 sec*	*20 sec*
A65							
1 sec	0.84						
2 sec	*0.86*	0.82					
3 sec	*0.78*	*0.82*	*0.83*				
5 sec	*0.74*	*0.76*	*0.82*	0.86			
10 sec	*0.72*	*0.74*	*0.80*	0.87	0.71		
15 sec	*0.72*	*0.77*	*0.82*	0.87	0.76	0.84	
20 sec	*0.72*	*0.76*	*0.82*	0.82	0.81	0.85	0.84
T420							
1 sec	*0.9*						
2 sec	*0.74*	*0.79*					
3 sec	*0.77*	*0.78*	*0.81*				
5 sec	0.76	0.73	0.78	0.51			
10 sec	0.59	0.55	0.59	0.6	0.59		
15 sec	0.63	0.64	0.65	0.67	0.59	0.53	
20 sec	0.62	0.63	0.69	0.7	0.53	0.53	0.62
A310							
1 sec	*0.67*						
2 sec	*0.67*	*0.69*					
3 sec	*0.7*	*0.67*	*0.62*				
5 sec	0.55	0.57	0.68	0.63			
10 sec	0.63	0.62	0.67	0.74	0.86		
15 sec	0.65	0.68	0.72	0.78	0.86	0.81	
20 sec	0.66	0.7	0.73	0.8	0.87	0.81	0.78

3.2.4. Effect of length of video recording and camera type on the relationship between IRT and rectal temperature

Based on previous results on the statistic calculated (e.g. quantiles) and the length of time (number of data points) used to calculate the

Table 5
Pearson correlations between the IRT temperatures of cattle with any two non-overlapping data time chunks for the same animal (1, 2, 3, 5, 10, 15 and 20 s) using the 99th quantile summary statistics.

	1 sec	2 sec	3 sec	5 sec	10 sec	15 sec	20 sec
A65							
1 sec	0.85						
2 sec	0.86	0.82					
3 sec	0.78	0.83	0.84				
5 sec	0.74	0.76	0.83	0.86			
10 sec	0.73	0.75	0.81	0.87	0.72		
15 sec	0.72	0.77	0.83	0.87	0.78	0.84	
20 sec	0.71	0.76	0.8	0.82	0.825	0.85	0.845
T420							
1 sec	0.88						
2 sec	0.75	0.79					
3 sec	0.78	0.79	0.81				
5 sec	0.77	0.69	0.75	0.48			
10 sec	0.58	0.53	0.57	0.6	0.57		
15 sec	0.6	0.6	0.61	0.63	0.58	0.47	
20 sec	0.57	0.57	0.63	0.64	0.49	0.47	0.6
A310							
1 sec	0.67						
2 sec	0.67	0.69					
3 sec	0.69	0.67	0.61				
5 sec	0.55	0.57	0.68	0.63			
10 sec	0.64	0.63	0.68	0.74	0.86		
15 sec	0.65	0.68	0.73	0.79	0.86	0.8	
20 sec	0.66	0.69	0.73	0.8	0.86	0.8	0.77

Table 6
Pearson correlations between the IRT temperatures of cattle with any two non-overlapping data time chunks for the same animal (1, 2, 3, 5, 10, 15 and 20 s) using the smoothed maximum summary statistics.

	1 sec	*2* sec	*3* sec	5 sec	10 sec	15 sec	20 sec
A65							
1 sec	0.85						
2 sec	*0.86*	0.82					
3 sec	*0.78*	*0.83*	*0.84*				
5 sec	*0.74*	*0.76*	*0.83*	0.86			
10 sec	*0.73*	*0.75*	*0.82*	0.87	0.73		
15 sec	*0.71*	*0.77*	*0.83*	0.87	0.79	0.84	
20 sec	*0.69*	*0.76*	*0.78*	0.82	0.84	0.85	0.85
T420							
1 sec	*0.86*						
2 sec	*0.75*	*0.78*					
3 sec	*0.78*	*0.79*	*0.8*				
5 sec	0.78	0.64	0.71	0.45			
10 sec	0.56	0.5	0.55	0.6	0.54		
15 sec	*0.57*	0.55	0.57	0.58	0.56	0.4	
20 sec	0.52	0.51	0.56	0.58	0.44	0.41	0.58
A310							
1 sec	*0.67*						
2 sec	*0.67*	*0.68*					
3 sec	*0.68*	*0.67*	*0.6*				
5 sec	0.55	0.56	0.68	0.63			
10 sec	0.64	0.64	0.68	0.74	0.86		
15 sec	0.65	0.68	0.73	0.79	0.85	0.79	
20 sec	0.65	0.69	0.73	0.79	0.84	0.78	0.76

statistics, we have combined the most accurate statistic and length of time to assess the relationship between ocular IRT and rectal temperature. Table 7 shows that shortening the length of time to obtain the summary statistics from all data available from each animal results in a reduction of the strength of the correlation for all 3 cameras and all summary statistics. The average number of frames for all data was 1244 frames for A65, 2522 for T420, and 1467 for A310 (data not shown). Differences between cameras also existed, with the A65 showing a large reduction in the strength of the correlation between IRT and rectal

Table 7
Pearson correlation coefficients between rectal and IRT temperature of the eye of cattle using the 90, 95, 97 and 99th quantiles as calculated from the rolling median and the 1-second rolling median maximum IRT using all data available, i.e. 1, 2, 3, 5 and 10-seconds chunks of data.

	1 secs	*2 secs*	*3 secs*	*5 secs*	*10* sec	*All data*
A65						
90th quantile	*0.00*	*0.05*	*0.13*	*0.3******	*0.29******	0.43***
95th quantile	−0.01	*0.05*	*0.15*	*0.3******	*0.29******	0.44***
97th quantile	−0.01	*0.05*	*0.16*	*0.3******	*0.31******	0.45***
99th quantile	*−0.01*	*0.05*	*0.17**	*0.3******	*0.31******	0.47***
rolling median maximum	−0.01	*0.05*	*0.17**	*0.3******	*0.3******	0.41***
T420						
90th quantile	*0.14*	*0.17**	*0.24****	*0.32******	*0.37******	0.37***
95th quantile	0.13	*0.17**	*0.25****	*0.29****	*0.31******	0.38***
97th quantile	*0.13*	*0.17**	*0.25****	*0.28****	*0.28****	0.4***
99th quantile	*0.13*	*0.17**	*0.24****	*0.28****	*0.28****	0.35***
rolling median maximum	*0.13*	*0.17**	*0.24****	*0.27****	*0.27****	0.32***
A310						
90th quantile	*0.39******	*0.35******	*0.36******	*0.36******	*0.4******	0.39***
95th quantile	0.39***	*0.36******	*0.37******	*0.36******	*0.38******	0.44***
97th quantile	*0.39******	*0.37******	*0.38******	*0.37******	*0.37******	0.46***
99th quantile	*0.39******	*0.37******	*0.38******	*0.38******	*0.37******	0.56***
rolling median maximum	*0.40******	*0.37******	*0.38******	*0.38******	*0.38******	0.57***

temperature when summary statistics are calculated over shorter time periods. A smaller reduction was reported for the T420, with the correlation coefficient being not significantly different to zero when only 1-second of data was used. In contrast, the A310 showed a similar correlation coefficients independently of the length of time used to calculate the summary statistic (Table 7).

4. Discussion

Several studies have previously been conducted to evaluate the ability of IRT to reflect the internal body temperature in animals (George et al., 2014; Hoffmann et al., 2013; Knížková et al., 2007). Very few studies used video IRT and defined the quality of the infrared data used (Hoffmann et al., 2013; Stewart et al., 2008). Using IRT video cameras could lead to better results in comparison to using solely still images, because using video allows continuous monitoring of animals as opposed to a single time point measurement. Hence, video IRT may provide more accurate temperature measurement as it is measuring the temperature of the animal multiple times per second, as opposed to a single image. Results of the present study confirm this because, IRT from the C2 camera showed lower correlation with rectal temperature compared to the video cameras. The advantage of video cameras is that they can record at high frame rates (up to 24 frames per second in the present study), which may be of value for animals that move fast through the ROI, blink or quickly react to external stimuli. However, the challenge with video IRT data collected at high frequencies is to process the video imagery to extract a temperature value that is most indicative of core body temperature.

Data collected at the commercial abattoir of the present study showed, that IRT data from video cameras is very variable and noisy depending on whether the animal was within the region of interest or not, and on the anatomical part of the animal within the ROI. Experiment 1 was conducted to help understand the reasons for this large variability under commercial abattoir settings and revealed three distinct different populations of IRT temperature. These distinct populations of data points with different means comprise mixed distributions with each population arising from different objects within the ROI. The animal's eye showed the highest temperature because it contains superficial blood vessels that are located near the surface and represent the closest temperature to internal core body temperature (Bartolomé et al., 2013; Stewart et al., 2008). This explains the reason for the appearance of the population with higher temperatures which contained the eye (ocular region). In contrast, the skin of the animal is insulated by hair, and blood vessels are deeper underneath the skin which therefore results in the lower IRT body temperatures (Kotrba et al., 2007). The appearance of mixed distributions is important because it could allow fitting probability density functions to obtain thresholds points above or below, which, a data point is assigned to one of the three populations with a minimum miss assignment rate. Such methodology has already been successfully used on biological cattle data for unsupervised classification of data points (González et al., 2015). Nevertheless, it is important to note that the intersect point between any of the two populations (eye and body, body and facilities) may vary for every dataset. This could be due to differences in ambient environmental conditions, the animals, experimental conditions (e.g. shade, direct sunlight, wind speed) and setup of cameras (distance, background interference) (Bernard et al., 2013; Church et al., 2014; Westermann et al., 2013). The setup and methodology of IRT studies must be carefully controlled to decrease the effect of these factors, as there is no correction model available to eliminate or reduce the effect of these factors at present. This may be particularly challenging under fast paced commercial conditions (Minkina and Dudzik, 2009).

The present study also demonstrated that pre-processing of infrared video data by calculating the rolling median and quantiles is required to obtain accurate measurements of body temperature of cattle. Animals are known to be more difficult for capturing good quality IRT data in comparison to humans, due to their unpredictable movements. When animals are moving through the ROI at high speeds, such as in the case of cattle exiting the crush or moving up the race before slaughter, cameras aren't able to obtain a focused image of the ROI. Cattle were recorded in the crush, under the cover of shade to avoid hot spots or artefacts on the animal during recording. By using a well-defined ROI, the occurrence of these outliers is limited, however, these can still appear when the animals move. Therefore, these occurrences need to be filtered out manually by disregarding such frames for analysis (Minkina and Dudzik, 2009), or using the summary statistics used in the present study (1-second rolling median or quantiles), or using automatic eye tracking software that detect, track and measure the temperature of the ocular region of the eye of each animal from video IRT (Jaddoa et al., 2018). This could result in IRT data being free of outliers however, this has not been proven at present to the authors' best knowledge.

In the present study, the data processing of calculating summary statistics and watching the videos to determine when the animal enters and leaves the ROI, used in the present study improved the correlations between IRT and rectal temperature compared to the raw unprocessed data. Most infrared studies in animals, use the raw maximum temperature for final analysis (Bartolomé et al., 2013; Hoffmann et al., 2013; Stewart et al., 2007) whereas others used the average of all pixels in the selected ROI (Šabec and Lazar, 1990; Traulsen et al., 2010). However, the former method was less accurate in the present study (particularly for the cameras with no fixed focus) and the latter has the limitation that it requires a precise definition of the ROI in regards to its size and position.

There is limited literature describing the most appropriate way to handle and analyse IRT animal data, particularly from IRT videos collected at high frequency. A study in humans (Ludwig et al., 2014) described and evaluated 3 different methods of IRT analysis. The methods of analysis consisted of 1) defining a ROI selected by the operator and calculating an arithmetic mean of all pixels within that ROI, 2) defining a ROI selected by the operator, followed by the software selecting an area of 5×5 pixels around the pixel with the maximum temperature and then averaging those 5 'hottest' pixels; and 3) defining a larger ROI to include background facilities in the ROI, then calculating the arithmetic mean. Results from that study found, that method 2 performed best in terms of asymmetry and thermal patterns. However, this processing method would not be possible for video IRT of animals due to 1) animals are moving at a very fast pace and rarely completely still 2) the definition of the ROI carries certain subjectivity and 3) asymmetry of animals and thermal patterns would be very difficult in a commercial setting. The smoothed maximum IRT temperature used to calculate quantiles (q50-q99) in the present study showed the highest correlation with rectal temperature in the A310 camera. In Experiment 1, maximum IRT temperature from raw data showed the highest temperature, the maximum of the 1-second rolling median showed the second highest, and temperature decreased with lower quantiles. The smoothed maximum, the q97 and q99 showed the highest correlation with rectal temperature on average across cameras and thus, these summary statistics seem the most suitable for data processing and analysis. The raw maximum had a lesser correlation with rectal temperature and is likely to be due to outliers that can occur regularly in IRT series as previously discussed. The raw maximum was particularly poor in the T420 camera, probable reasons for this could be that these cameras have greater sensitivity, resolution, frame rate and auto-focus rate. However, the raw maximum showed similar correlation coefficients compared to the upper quantiles for the A65. This could be due to the fact this camera has a fixed focus setting and so the camera is not continuously refocussing, it remains fixed for the entire recording period. Thus, the final data does not contain refocussing issues as the other two cameras resulting in more stable temperature measurements over time. This fixed focus may be more suitable for use in commercial conditions where animals come into and outside the ROI frequently. However, the A65 showed the lowest correlations with rectal temperatures when using recordings for very short periods of time (1 s), followed by the T420 and then lastly the A310 being least affected by the length of the recording. This was interesting because the A65 had the highest resolution but, a larger error of accuracy than the other cameras. These findings together with the fact that using raw data did not affect the strength of the correlation between IRT and rectal temperature for the A65 suggest, that accuracy and auto-focus capability has a greater effect on image quality in these conditions than differences in resolution.

As is the case under most commercial conditions, animals move at fast speed which may not allow much time for IRT data to be captured. Abattoirs cannot afford to be slowed down and animals need to be moved at a continuous and fast pace, and IRT data must be collected in very short time frames. In addition, IRT measurements on the same animal measured for different lengths of time and at different points in time, should be repeatable. The high average correlation coefficients reported between any 2 non-overlapping chunks of data ($r = 0.72$) indicate that measurements are repeatable and not largely affected by the length of time the animal was in the ROI. This is an important finding that supports the suitability of video IRT for applications in animals under commercial conditions. To our knowledge, there has not been much research surrounding the minimum time needed to obtain an accurate IRT reading for fast moving animals.

It's important to note, that even though results from the present study revealed similar correlations between IRT and rectal temperature in cattle as other studies (George et al., 2014; Hoffmann et al., 2013; Salles et al., 2016), there is currently no gold standard for measuring internal core body temperature to compare against IRT. Most frequently, rectal temperature has been assumed as the best indicator of core body temperature (Hanneman et al., 2004). Rectal temperature is a single measurement taken at one time point and is not always indicative of the animals' overall physiological status. Using IRT of the ocular region of the eye, with its high supply of blood capillaries at the surface, allows for quick changes in the animals' temperature to be captured, which rectal temperature may miss as previously demonstrated by Sellier et al. (2014). This could explain the weak correlations between IRT and rectal temperature reported in the present study. However, previous studies have achieved stronger correlations (0.77) with IRT and internal loggers that continuously record internal body temperature (George et al., 2014; Lee et al., 2016). It has also been stated that IRT is poor at distinguishing healthy animals but rather works well at detecting animals that are clinically different such as ill, injured or stressed (Schaefer et al., 2004).

The manual filtering and data processing is time consuming and requires researchers to watch and analyse the videos in a very detailed manner, an unviable approach for an automatic monitoring system. Therefore, the above-mentioned techniques are more applicable in research rather than a practical, commercially viable situation. For IRT data to be used successfully with accurate results, in real time under a commercial setting, a simpler, automatic method of data processing is needed. The initial smoothing of the raw IRT data using a rolling median over 1 s and summary statistics (e.g. quantiles) could be useful for commercial applications. The smoothing method could be calculated in real time and seems effective at smoothing spikes (hot artefacts and/or camera glitches) and troughs (eye or animal out of ROI). The rolling median was used instead of a rolling average as it was shown to have the tightest distribution and the largest noise-reducing effect in other studies (Henrik and Jonathon, 2002). However, smoothing may not be enough to remove all outliers, particularly in long periods of spikes or troughs. These longer periods of spikes or troughs in temperature are more likely to be removed with summary statistics such as the quantiles. However, this method still requires watching the videos and indicating when an animal enters and leaves the ROI. Therefore, automatic eye tracking software for IRT data that can handle animals moving at a faster pace would be ideal for adopting the quantile processing approach.

5. Conclusions

We have shown that video IRT has the potential to measure body temperature from animals in real time with potential applications to remotely measure animal health and welfare, and allow making informed decisions under commercial conditions. The present study demonstrate that video IRT data requires extensive pre-processing and algorithms to obtain summary statistics applicable to animals moving at fast paces and eliminate outliers or unrealistic measurements. Recommendations from the present study encourages pre-processing of IRT data by calculating summary statistics for each animal before analysis, including a 1-second rolling median and the 97th or 99th quantiles due to their stronger correlation with rectal temperature. Measurements on the same animal are repeatable over periods of varying time length, however, shorter time periods could jeopardise the correlation between IRT and biological data from some cameras depending on frame rate, resolution and accuracy.

Acknowledgements

This work was supported by Meat and Livestock Australia, Australian Meat Processor Corporation and The University of Sydney. The authors would like to thank the Sydney University farm staff for their assistance handling the cattle during the trial and to the abattoir staff for aiding the collection of infrared data.

Appendix A. Supplementary material

Supplementary data to this article can be found online at https://doi.org/10.1016/j.compag.2019.105019.

References

Arce, G.R., 2005. Nonlinear Signal Processing: A Statistical Approach. John Wiley & Sons.
Bartolomé, E., Sánchez, M.J., Molina, A., Schaefer, A.L., Cervantes, I., Valera, M., 2013. Using eye temperature and heart rate for stress assessment in young horses competing in jumping competitions and its possible influence on sport performance. Animal 7, 2044–2053.
Bernard, V., Staffa, E., Mornstein, V., Bourek, A., 2013. Infrared camera assessment of skin surface temperature–effect of emissivity. Phys. Med. 29, 583–591. https://doi.org/10.1016/j.ejmp.2012.09.003.
Burfeind, O., Von Keyserlingk, M.A.G., Weary, D.M., Veira, D.M., Heuwieser, W., 2010. Repeatability of measures of rectal temperature in dairy cows. J. Dairy Sci. 93, 624–627.
Chang, W., Cheng, J., Allaire, J., Xie, Y., McPherson, J., 2018. Shiny. Web application framework for R. R package version [1.00]. 2017.
Church, J.S., Hegadoren, P.R., Paetkau, M.J., Miller, C.C., Regev-Shoshani, G., Schaefer, A.L., Schwartzkopf-Genswein, K.S., 2014. Influence of environmental factors on infrared eye temperature measurements in cattle. Res. Vet. Sci. 96, 220–226. https://doi.org/10.1016/j.rvsc.2013.11.006.
Gariepy, C., Amiot, J., Nadai, S., 1989. Ante-mortem detection of PSE and DFD by infrared thermography of pigs before stunning. Meat. Sci. 25, 37–41. https://doi.org/10.1016/0309-1740(89)90064-8.
George, W.D., Godfrey, R.W., Ketring, R.C., Vinson, M.C., Willard, S.T., 2014. Relationship among eye and muzzle temperatures measured using digital infrared thermal imaging and vaginal and rectal temperatures in hair sheep and cattle. J. Anim. Sci. 92, 4949–4955. https://doi.org/10.2527/jas.2014-8087.
González, L.A., Bishop-Hurley, G.J., Handcock, R.N., Crossman, C., 2015. Behavioral classification of data from collars containing motion sensors in grazing cattle. Comput. Electron. Agric. 110, 91–102.
Hanneman, S.K., Jesurum-Urbaitis, J.T., Bickel, D.R., 2004. Comparison of methods of temperature measurement in swine. Lab. Anim. 38, 297–306.
Henrik, C., Jonathon, P.P., 2002. Empirical Evaluation Methods in Computer Vision. World Scientific.
Herborn, K.A., Graves, J.L., Jerem, P., Evans, N.P., Nager, R., McCafferty, D.J., McKeegan, D.E.F., 2015. Skin temperature reveals the intensity of acute stress. Physiol. Behav. 152, 225–230. https://doi.org/10.1016/j.physbeh.2015.09.032.
Hoffmann, G., Schmidt, M., Ammon, C., Rose-Meierhofer, S., Burfeind, O., Heuwieser, W., Berg, W., 2013. Monitoring the body temperature of cows and calves using video recordings from an infrared thermography camera. Vet .Res. Commun. 37, 91–99. https://doi.org/10.1007/s11259-012-9549-3.
Jaddoa, M., Al-Jumaily, A., Gonzalez, L., Cuthbertson, H., 2018. Automatic Eyes Localization in Thermal Images for Temperature Measurement in Cattle. https://doi.org/10.1109/ISKE.2017.8258765.
Kessel, L., Johnson, L., Arvidsson, H., Larsen, M., 2010. The relationship between body and ambient temperature and corneal temperature. Invest. Ophthalmol. Vis. Sci. 51, 6593–6597.
Knížková, I., Kunc, P., Gürdil, G.A.K., Pinar, Y., Selvi, K.C., 2007. Applications of infrared thermography in animal production. J. Fac. Agric. 22, 329–336.
Koltes, J.E., Koltes, D.A., Mote, B.E., Tucker, J., Hubbell III, D.S., 2018. Automated collection of heat stress data in livestock: new technologies and opportunities. Transl. Anim. Sci. 2, 319–323.
Kotrba, R., Knížková, I., Kunc, P., Bartoš, L., 2007. Comparison between the coat temperature of the eland and dairy cattle by infrared thermography. J. Therm. Biol. 32, 355–359.
Lahiri, B.B., Bagavathiappan, S., Jayakumar, T., Philip, J., 2012. Medical applications of infrared thermography: a review. Infrared Phys. Technol. 55, 221–235.
Lee, Y., Bok, J.D., Lee, H.J., Lee, H.G., Kim, D., Lee, I., Kang, S.K., Choi, Y.J., 2016. Body temperature monitoring using subcutaneously implanted thermo-loggers from Holstein steers. Asian-Australas. J. Anim. Sci. 29, 299–306. https://doi.org/10.5713/ajas.15.0353.
Ludwig, N., Formenti, D., Gargano, M., Alberti, G., 2014. Skin temperature evaluation by infrared thermography: Comparison of image analysis methods. Infrared Phys. Technol. 62, 1–6. https://doi.org/10.1016/j.infrared.2013.09.011.
Mccafferty, D.J., 2007. The value of infrared thermography for research on mammals: previous applications and future directions. Mamm. Rev. 37, 207–223.
McManus, C., Tanure, C.B., Peripolli, V., Seixas, L., Fischer, V., Gabbi, A.M., Menegassi, S.R.O., Stumpf, M.T., Kolling, G.J., Dias, E., Costa, J.B.G., 2016. Infrared thermography in animal production: An overview. Comput. Electron. Agric. 123, 10–16. https://doi.org/10.1016/j.compag.2016.01.027.
Minkina, W., Dudzik, S., 2009. Infrared Thermography: Errors and Uncertainties. John Wiley & Sons.
Naylor, J.M., Streeter, R.M., Torgerson, P., 2012. Factors affecting rectal temperature measurement using commonly available digital thermometers. Res. Vet. Sci. 92, 121–123.
R Core Team, 2015. R: A Language and Environment for Statistical Computing.
Ratner, B., 2009. The correlation coefficient: Its values range between $+1/-1$, or do they? J. Target. Meas. Anal. Mark. 17, 139–142. https://doi.org/10.1057/jt.2009.5.
Rose-Dye, T.K., Burciaga-Robles, L.O., Krehbiel, C.R., Step, D.L., Fulton, R.W., Confer, A.W., Richards, C.J., 2011. Rumen temperature change monitored with remote rumen temperature boluses after challenges with bovine viral diarrhea virus and Mannheimia haemolytica. J. Anim. Sci. 89, 1193–1200.
Šabec, D., Lazar, P., 1990. Initial results of measuring the skin temperature over the hock joint of pigs with deforming osteoarthritis, by using an infrared thermometer. Dtsch. Tierarztl. Wochenschr. 97, 43–44.
Salles, M.S., da Silva, S.C., Salles, F.A., Roma Jr., L.C., El Faro, L., Bustos Mac Lean, P.A., Lins de Oliveira, C.E., Martello, L.S., 2016. Mapping the body surface temperature of cattle by infrared thermography. J. Therm. Biol. 62, 63–69. https://doi.org/10.1016/j.jtherbio.2016.10.003.
Schaefer, A.L., Cook, N., Tessaro, S.V., Deregt, D., Desroches, G., Dubeski, P.L., Tong, A.K.W., Godson, D.L., 2004. Early detection and prediction of infection using infrared thermography. Can. J. Anim. Sci. 84, 73–80.
Sellier, N., Guettier, E., Staub, C., 2014. A review of methods to measure animal body temperature in precision farming. Am. J. Agric. Sci. Technol. 2, 74–99.
Stewart, M., Schaefer, A.L., Haley, D.B., Colyn, J., Cook, N.J., Stafford, K.J., Webster, J.R., 2008. Infrared thermography as a non-invasive method for detecting fear-related responses of cattle to handling procedures. Anim. Welf. 17, 387–393.
Stewart, M., Webster, J.R., Schaefer, A.L., Cook, N.J., Scott, S.L., 2005. Infrared thermography as a non-invasive tool to study animal welfare. Anim. Welf. 14, 319–325.
Stewart, M., Webster, J.R., Verkerk, G.A., Schaefer, A.L., Colyn, J.J., Stafford, K.J., 2007. Non-invasive measurement of stress in dairy cows using infrared thermography. Physiol. Behav. 92, 520–525. https://doi.org/10.1016/j.physbeh.2007.04.034.
Traulsen, I., Naunin, K., Mueller, K., Krieter, J., 2010. Application of infrared thermography to measure body temperature of sows. Züchtungskunde 82, 437–446.

Tuszynski, J., 2019. CA Tools: Tools: moving window statistics, GIF, Base64, ROC AUC, etc.
Usamentiaga, R., Venegas, P., Guerediaga, J., Vega, L., Molleda, J., Bulnes, F., 2014. Infrared thermography for temperature measurement and non-destructive testing. Sensors 14, 12305–12348.
Wacker, C.B., Rojas, A.D., Geiser, F., 2012. The use of small subcutaneous transponders for quantifying thermal biology and torpor in small mammals. J. Therm. Biol. 37, 250–254.
Westermann, S., Buchner, H.H.F., Schramel, J.P., Tichy, A., Stanek, C., 2013. Effects of infrared camera angle and distance on measurement and reproducibility of thermographically determined temperatures of the distolateral aspects of the forelimbs in horses. J. Am. Vet. Med. Assoc. 242, 388–395.
Wickham, H., 2016. Ggplot2: Elegant Graphics for Data Analysis. Springer.
Wolfe, W.L., 1965. Handbook of Military Infrared Technology. MICHIGAN UNIV ANN ARBOR.